Thermoelectric Textiles for Body Heat Regulation and Energy Harvesting

Madison Miller, Department of Materials Science and Engineering, University of Florida
NNCI REU Site: Georgia Institute of Technology
Principal Investigator: Dr. Blair Brettmann, Department of Materials Science and Engineering, Department of Chemical and Biomolecular Engineering, Georgia Tech
Mentor: Elena Ewaldz, Department of Materials Science and Engineering, Georgia Tech

Abstract: Thermoelectric textiles are able to take thermal energy and convert it to electrical energy and have potential for use in numerous applications, from charging portable devices to being used for body heat regulation. Electrospinning conductive polymer solutions into nanofiber mats has been shown to be a successful technique for creating these thermoelectric textiles. This process creates conductive fiber mats, but their conductivity has not previously been extensively compared to that of thin films made using the same conductive polymer solutions. This paper presents a method for increasing the conductivity of electrospun PEDOT:PSS fiber mats via thermal treatments that have previously shown success when used for thin films. Treatments were conducted at 100°, 150°, and 200°C, with all samples showing an increase in conductivity regardless of treatment time or temperature. The best results were obtained for the treatment at 200°C for 10 minutes, with a 558% increase in fiber conductivity. The use of thermal treatments shows promise as a method of increasing conductivity of electrospun PEDOT:PSS fibers for their use in thermoelectric textiles.

I. Introduction and Motivation

As electronics are becoming increasingly compact, there is an increasing interest in creating wearable electronics. Traditional electronic materials such as silicon and germanium are stiff and heavy, while wearable electronics are both flexible and lightweight. Previous research has shown that flexible electronic materials exhibit their best performance when in the flexible range. This property of wearable electronics provides the opportunity to create devices that are not able to be fabricated using traditional electronic materials due to their structural limitations. [1] Flexible electronic materials show potential for incorporation into textiles when used in combination with nanofiber fabrication processes, especially electrospinning.

One area of particular interest is the development of thermoelectric textiles, which can convert thermal energy to electrical energy. Thermoelectric textiles require both a p- and n-type semiconductor, which allows for voltage to be generated when the textile experiences a temperature change. The effectiveness of the thermoelectric is dependent on the Seebeck coefficient of the material, the operating temperature, and the thermal and electrical conductivities of the materials. Conductive polymers are one of the prime areas of research for use in thermoelectric textiles since they are flexible and exhibit similar performance to traditional electronic materials in lower temperature ranges. [2] When incorporated into clothing, these textiles would allow for the charging of portable devices such as smart phones and smart watches.

Previous success has been achieved with flexible devices developed via electrospinning [1], which is a process that creates a fiber mat that can act as a component of a thermoelectric textile. The electrospinning process allows for the creation of continuous nanofibers composed of either organic or inorganic materials. [3] The use of conductive polymers in electrospinning is optimal for the creation of thermoelectric textiles because the properties of the polymer can be easily modified in comparison to inorganic materials, and they have low thermal conductivities as well as adjustable surface properties via solution additives. [1] A thermoelectric textile requires the layering of p-type and n-type electrospun fiber mats. [2] In order to

create an effective electrospun p-type component of a thermoelectric textile, this research focused on enhancing the conductivity of fiber mats using thermal treatments that have been shown to improve conductivity in thin films [4]. A 1.3 wt% dispersion in water of PEDOT:PSS, a molecule complex, was used to create a solution containing 1 wt% of 2 million g/mol molecular weight poly(ethylene oxide) in PEDOT:PSS. This solution was used for the electrospinning process. Both the PEDOT:PSS and the poly(ethylene oxide) were purchased from Sigma Aldrich.

II. Experimental Conditions

A. Sample Creation Process

An overview of the electrospinning process is shown in Figure 1. The solution is loaded into a syringe that is placed in a syringe pump that can be used to control the flow rate of the solution. A high voltage is applied to the needle that the solution is coming out of, and a conductive collection plate is grounded. In order to get the formation of a Taylor cone with one jet, the surface tension of the solution must be balanced with the electric field. The surface tension is impacted by solution additives as well as the flow rate, while the electric field is impacted by the applied voltage and the distance between the needle and the collection plate. These parameters vary depending on the solution used as well as environmental conditions such as temperature and humidity, which have a large impact on the final morphology of the fibers. [3] A higher humidity can lead to fibers clumping and the fiber mat behaving like a film rather than a textile. An example of smooth fibers compared to clumped fibers can be seen in Figures 2 and 3.

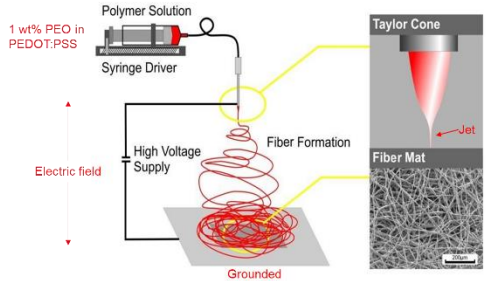

Figure 1: An overview of the electrospinning process [5], annotations added by author.

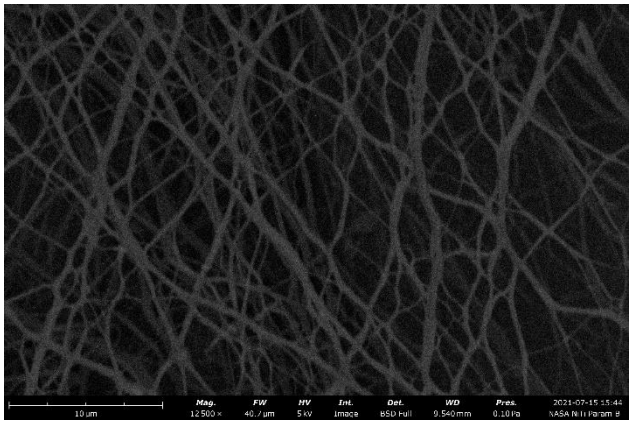

Figure 2: An SEM image of smooth electrospun PEDOT:PSS fibers.

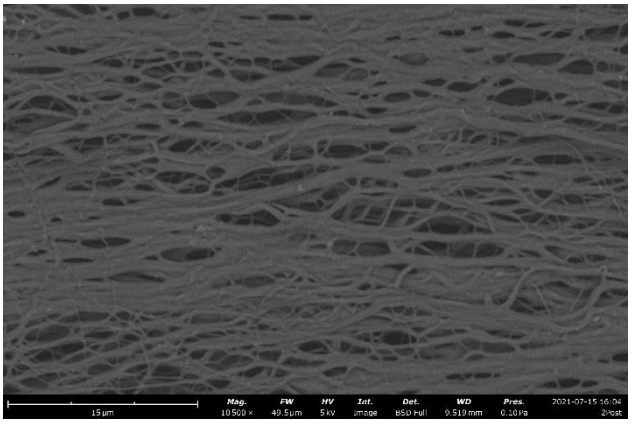

Figure 3: An SEM image of clumped electrospun PEDOT:PSS fibers.

The PEDOT:PSS solution was electrospun directly onto silicon wafers to create a total of 7 samples. After a sufficient layer of fibers was spun on the wafers, e-beam evaporation was used to deposit a 100 nm layer of gold on the surface of the fibers for use in resistance measurements. A shadow mask was used during this process to

create the pattern on the surface that was used for 4-point probe measurements, shown in Figure 4.

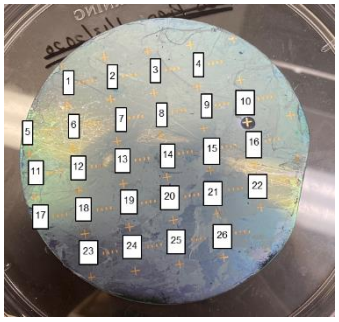

Figure 4: An electrospun fiber mat on a silicon wafer with gold deposited on the surface and the 26 4-point probe points used for measurement labeled.

B. Resistance Data Collection

A 4-point probe was used to collect resistance data for each of the fiber mats at each of the 26 points labeled in Figure 4. Three measurements were taken at each of these points both before and after thermal treatment. Some samples did not have fibers collected on some of the points, in which case measurements were not recorded at that point.

C. Thickness Measurements

In order to determine the conductivity of the fibers, the thickness of the fiber mat is needed as shown in the following derivation, where R is resistance, ρ is resistivity, L is length, A is cross-sectional area, σ is conductivity, and t is thickness: $R = \frac{\rho L}{A} \rightarrow \sigma = \frac{1}{\rho} \rightarrow \sigma = \frac{L}{RA} = \frac{1}{Rt}$. Contact profilometry was attempted for one of the samples but damaged the sample because the stylus dragged the fibers, which also led to an inaccurate thickness measurement. The fiber mats were too thin to measure with optical microscopy, so optical profilometry was used to determine the thickness of the mats. One thickness measurement was taken for most of the samples in the area that seemed to be of average thickness. On samples with obvious variations in thickness across the wafer, multiple measurements were taken. An example of the data collected from the optical profilometer is shown in Figures 5 and 6.

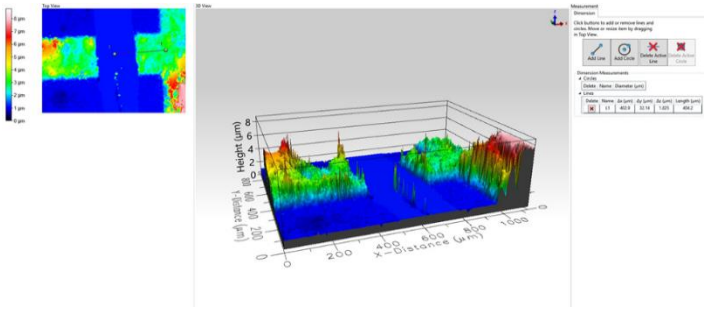

Figure 5: A side view of one of the scans obtained using optical profilometry, showing the height of the fiber mat. The green areas are most representative of the average fiber mat thickness.

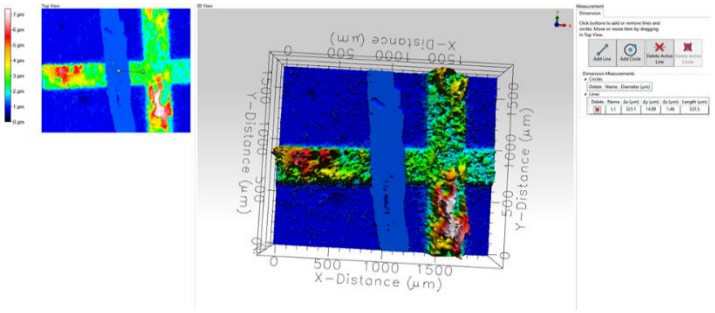

Figure 6: A top view of one of the scans obtained using optical profilometry. The light blue line shows the scratch made on the surface that was used as a reference point for the thickness measurements.

A scratch was made on the surface of the wafer on one of the gold plus signs to provide a reference point. The difference between this flat surface and the green areas in the scan, which are representative of the average fiber mat height, were used to determine the thickness of the fiber mat. The thickness of the gold layer, 100 nm, was subtracted from this value to get a final thickness measurement for use in conductivity calculations.

D. Thermal Treatments

Thermal treatments were conducted at 100°, 150°, and 200°C for 10 minutes and 30 minutes. An additional treatment was conducted at 200°C for 20 minutes due to a large difference in conductivity increase between the treatments for 10 minutes and 30 minutes at that temperature. After the thermal treatments, the resistance at each of the 26 points labelled in Figure 4 was recorded again for use in conductivity calculations.

III. Results and Discussion

After collecting three resistance measurements at each of the 26 points labelled in Figure 4 before and after the thermal treatments, the average resistance for each point was calculated. The mean resistance of all 26 points as well as the standard deviation for each sample was then calculated to determine outliers in the data using a z-score, where the z-score was equal to the average resistance at the respective point minus the overall mean resistance divided by the standard deviation. A z-score greater than 3 qualified the point as an outlier. These outliers were not used in subsequent calculations. The thickness measurements for each sample were then used to calculate the conductivity at each of the 26 points of the sample before and after thermal treatment using the following equation: $\sigma = \frac{1}{Rt}$, where R is the resistance and t is the thickness. The same thickness values were used for pre- and post-treatment conductivity calculations for each sample. The percent difference between the pre- and post-treatment conductivity values were then calculated for each of the 26 points on each sample. The average of these percent differences was calculated for each treatment and these averages are shown in Figures 7 and 8.

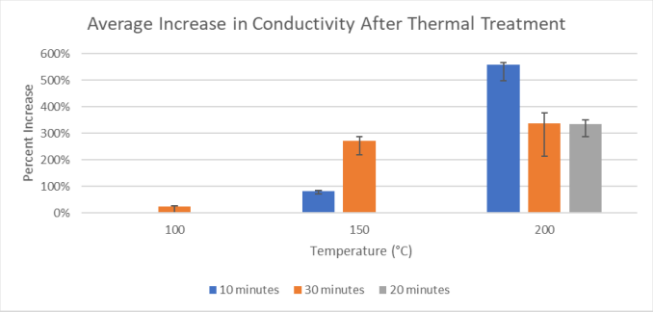

Figure 7: A comparison of the percent change in conductivity for each thermal treatment. No data is shown for the sample treated at 100°C for 10 minutes because the sample was damaged during contact profilometry.

Temperature/Time	10 minutes	20 minutes	30 minutes
100°C	--	--	24%
150°C	82%	--	272%
200°C	558%	334%	338%

Figure 8: The average percent increase in conductivity after thermal treatments. No data is shown for the sample treated at 100°C for 10 minutes because the sample was damaged during contact profilometry.

All of the samples showed an increase in conductivity after thermal treatment, with the best results being for the treatments conducted at 200°C. The treatments at 150°C showed a significant increase in conductivity from the 10 minute to the 30

minute treatment, which was not exhibited in the data for the treatments at 200°C. An additional treatment at 200°C for 20 minutes resulted in a similar percent increase in conductivity as the treatment for 30 minutes. Further treatments at this temperature, as well as at 100° and 150°C will be conducted in the future to determine if this is a definitive trend.

IV. Conclusions and Future Work

The results of the thermal treatments are promising for the development of electrospun thermoelectric textiles using PEDOT:PSS. All the treatments led to an increase in conductivity, with the best results being for the treatment conducted at 200°C at 10 minutes. The samples treated at 200°C for 20 minutes and 30 minutes showed similar increases in conductivity that were both less than that of the 10 minute treatment at 200°C. These samples still experienced a larger conductivity increase than the samples treated at 150°C. These treatments will need to be repeated for multiple samples to confirm these results. More treatments at these temperatures for longer periods of time will be conducted as well. In addition, scanning electron microscopy of cross sections of the samples will be used to confirm the thickness values obtained from the optical profilometry, which is a potential method for the measurement of electrospun fiber mat thicknesses.

V. Acknowledgements

NSF EEC 1757579, Leslie O'Neill, Dr. Quinn Spadola, Brettmann Lab, Stingelin Lab, Materials Innovation and Learning Laboratory, IEN/IMAT Materials Characterization Facility, IEN Micro/Nano Fabrication Facility, Georgia Tech Research Institute HIVES Program

VI. References

[1] B. Sun, Y. Long, Z. Chen, S. Liu, H. Zhang, J. Zhang, & W. Han, "Recent advances in flexible and stretchable electronic devices via electrospinning," *J. Mater. Chem. C*, 2014, DOI: 10.1039/c3tc31680g.

[2] A.K. Menon, O. Meek, A.J. Eng, & S.K. Yee, "Radial thermoelectric generator fabricated from n- and p-type conducting polymers," *J. Appl. Polym. Sci.*, 2017, DOI: 10.1002/app.44060.

[3] J.H. Yu, & G.C. Rutledge, "Electrospinning" in *Encyclopedia of Polymer Science and Technology*. Massachusetts Institute of Technology. John Wiley & Sons, Inc., 2007, ch. 1, pp. 1-20.

[4] H. Shi, C. Liu, Q. Jiang, & J. Xu, "Effective Approaches to Improve the Electrical Conductivity of PEDOT:PSS: A Review," *Adv. Electron. Mater.*, 2015, DOI: 10.1002/aelm.201500017.

[5] "Sketch of the Electrospinning Process," Oxolutia. https://www.oxolutia.com/technology/electrospinning/